ACS SENSORS

pubs.acs.org/acssensors Article

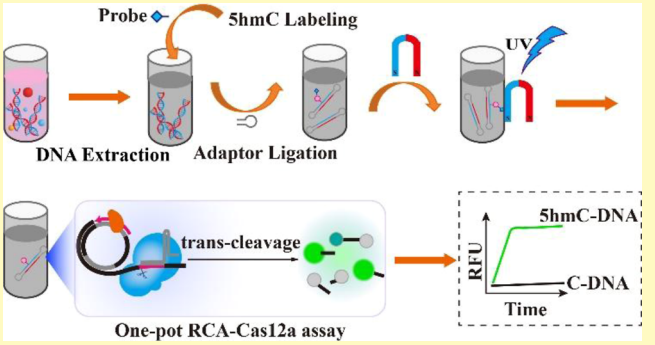
Chemical Modification Coupled with Isothermal CRISPR-Based Assay for Sensitive Detection of DNA Hydroxymethylation

Guangrong Zou,‖ Penglong Si,‖ Jiaqi Wang,‖ Meihua Yang, Jie Chen, Chaoxing Liu,* and Zhaofan Luo*

Cite This: *ACS Sens.* 2025, 10, 2073−2079 Read Online

ACCESS | Metrics & More | Article Recommendations | Supporting Information

ABSTRACT: 5-Hydroxymethylcytosine (5hmC) plays a key role in the DNA demethylation process and serves as a stable epigenetic marker in the human genome which is closely associated with disease progression, particularly in diabetes, colorectal cancer, and liver cancer. However, convenient and sensitive methods for detecting and quantifying 5hmC in the genome are scarce, especially in complex biological environments. Herein, a novel attempt at hypersensitive quantitative detection of 5hmC was presented. A multifunctional photosensitive probe was therefore introduced for specific labeling, enrichment, and elution of 5hmC-DNA. Combining with isothermal assay leveraging rolling circle amplification and Cas12a for accurate recognition, we achieved quantitative detection of 5hmC DNA in trace amounts at a level of 11 fM. Global 5hmC was measured in various biological samples using as little as 10 ng of input DNA by a real-time PCR instrument. The reported approach imposed no sequence restrictions, demonstrating promising potential for detecting modified bases in trace amounts of nucleic acids within complex environments, such as blood, urine, and saliva samples.



KEYWORDS: *DNA hydroxymethylation, Cas12a, isothermal amplification, chemical modification, detection*

Downloaded via SHANGHAI NORMAL UNIV on March 29, 2025 at 01:16:04 (UTC).
See https://pubs.acs.org/sharingguidelines for options on how to legitimately share published articles.

5-Hydroxymethylcytosine (5hmC) represents a vital epigenetic modification that exerts a profound impact on a vast array of biological processes, encompassing development and pathogenesis.[1,2] More significantly, 5hmC has also been demonstrated to affect the initiation and progression of diseases.[3,4] It shows a decreasing trend in both hematologic tumors and solid tumors compared to corresponding normal tissues,[5] such as melanoma,[6] colorectal cancer,[7,8] and hepatocellular carcinoma.[9] Therefore, 5hmC is a promising biomarker, which has great clinical utility value in the screening, diagnosis, and monitoring of diseases and tumors.[10]

Although 5hmC is abundantly present in human body as well as in plants and animals, exhibiting a tissue-specific distribution,[11] its content is 10−100 times less than 5-methylcytosine in the human genome.[12] Due to subtle differences among normal cytosine, 5-formylcytosine, 5-carboxylcytosine, and 5-methylcytosine and severe nontarget interference in diverse biofluids and cell types, there is an urgent need for robust, specific sensors and bioassays in order to facilitate the progression of clinically feasible modified nucleic acid biomarkers.

A number of techniques have been devised to detect and quantify 5hmC within the genomic landscape. Liquid chromatography−mass spectrometry is a traditional assay for precise quantification of 5hmC from various biological samples.[13,14] However, this method relies on large instruments and usually requires input DNA at the microgram scale. Enzyme-based techniques, such as employing radiolabeled glucose or endonucleases can also achieve the quantification of 5hmC in cells and tissues with sequence restrictions or radiation damage.[15,16] The 5hmC antibody detection assay is one kind of common methods, while sensitivity and specificity deeply depend on the purity and type of antibody.[17,18] Next-generation sequencing (NGS) techniques coupled with bisulfite conversion or TET enzyme oxidation can achieve quantitative detection of 5hmC, effectively.[19,20] Expensive instruments as well as professional bioinformation analysis are required in NGS. All in all, existing methods are general labor-intensive, expensive, high demanding amount input DNA, and fraught with potential errors, which hindered further clinical application.

RNA-guided CRISPR (clustered regularly interspaced short palindromic repeats) technologies are highly versatile tools for sequence-specific detection of DNA and RNA due to their high sensitivity and specificity.[21−23] The incredible system of CRISPR−Cas12a confers remarkable target recognition

Received: November 24, 2024
Revised: January 5, 2025
Accepted: February 25, 2025
Published: March 1, 2025

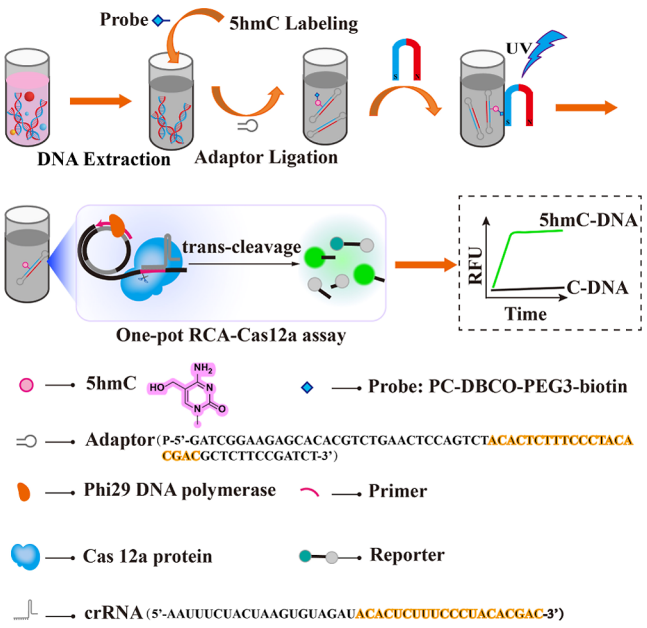


ACS Publications © 2025 American Chemical Society

accuracy and precision by binding with the Cas enzyme−crRNA complex. The enzymatic signal amplification is caused by collateral cleavage of the reporter by Cas12a protein, which is activated by target binding.[24,25] By fully leveraging this characteristic, assays that integrate CRISPR technologies with isothermal amplification have been developed for biomarker detection to achieve desirable sensitivity.[21,26−30] Precision, elevated sensitivity, ease of operation, cost-effectiveness, and the absence of precision instruments make these methods potential for clinical applications.

The current study demonstrates a novel strategy, the Chemically Assisted one-pot Isothermal CRISPR−Cas12a (CAICas12a) assay, to realize cost-effective and robust quantitation of 5hmC global level in low input with a handy instrument without sequence and site restrictions (Scheme 1).

Scheme 1. CAICas12a 5hmC Detection Assay[a]



[a]The workflow and key elements of the CAICas12a assay. First, extracted and fragmented 5hmC-DNA is labeled with probe PC-DBCO-PEG3-biotin and enriched by streptavidin magnetic beads, further eluted by short-duration 365 nm illumination. Then, the elution products are ligated to adaptors with hairpin structure to form ring templates for RCA. Finally, within the presence of primers, phi29 DNA polymerase, crRNA, Cas12a protein, and fluorescence reporter, the RCA products based on 5hmC-DNA can activate the cis-cleavage activity of Cas12a, as well as the trans-cleavage activity, digesting fluorescence reporter to release fluorescence signal.

CAICas12a assay employs a multifunctional chemical small molecule, PC-DBCO-PEG$_3$-biotin, for specific labeling and enrichment of 5hmC-N$_3$ sites, which are from 5hmC conversion by T4 β-glucosyltransferase (T4-β-GT). Additionally, the photolysis group (PC) in PC-DBCO-biotin facilitates specific elution following the 5hmC enrichment with biotin−streptavidin magnetic beads. Subsequently, the labeled and enriched 5hmC DNA is ligated with hairpin adaptors to enable cyclization. The resulting circular products were then utilized for rolling-circle amplification (RCA) in conjunction with Cas12a technology. By leveraging small-molecule labeling and enrichment for the first signal amplification, RCA for the second signal amplification and the collateral cleavage (trans-cleavage activity) of the reporter by the Cas12a protein activated once a target is bound for the third signal amplification, genomic 5hmC-DNA in cells and blood can be quantitatively detected with nanogram input.

RESULTS AND DISCUSSION

To develop an ultrasensitive chemical strategy combined with an isothermal amplification CRISPR-Cas12a assay to facilitate the 5hmC quantitative detection in genomic DNA, we used a commercial biotin molecule (PC-DBCO-PEG$_3$-biotin, Figure S1), which bears three essential moieties. The DBCO moiety served as the labeling group targeting for 5hmC, which was treated with glycosyltransferase. The biotin moiety acted as a high-affinity-binding motif for streptavidin, while the PC moiety acted as a photolysis group for elution following streptavidin enrichment. Shown as Figure 1A, we employed an enzyme-catalyzed coupling chemical click reaction for 5hmC labeling and enrichment.[31] An 80-mer duplex DNA, with one 5-hmC modification in each single strand, was prepared by polymerase chain reaction (PCR) as a model (Table S1). The use of UDP-6-N$_3$-Glu as a cofactor enables T4-β-GT to catalyze the transfer of a glucose moiety from UDP-6-N$_3$-Glu to the hydroxyl group of 5-hmC, yielding β-glucosyl-5-hydroxymethyl-cytosine (5hmC-N$_3$) in duplex DNA.[31] This product could then undergo a copper-free catalytic chemical click reaction with the DBCO group occurring in PC-DBCO-PEG$_3$-biotin, thus ultimately yielding biotin-PC-5hmC-DNA. The biotin-PC-5hmC-DNA produced contained a biotin moiety, allowing for specific enrichment through SA magnetic beads and achieving specific elution by UV light, conveniently. We validated this process by 18% denatured polyacrylamide gel with 20 bp 5hmC-DNA (Figure 1B) and confirmed the accuracy of the product through mass spectrometry (Figures S2 and S3). Besides, we also analyzed the chemical labeling efficiency of 5hmC-DNA with one or multiple 5hmC sites (Figure S4). It was observed that UDP-6-N$_3$-Glu and PC DBCO-PEG$_3$-biotin effectively and specifically labeled 5hmC-DNA, with only 30 s required for complete photolysis of 5hmC-DNA. The enrichment efficiency of 5hmC-DNA by this method was verified by qPCR. As illustrated in Figure 1C, the method demonstrated an ability to enrich 5hmC-DNA by up to 1289.1-fold. Overall, Figures 1, S2, and S3 confirmed that our improved method was quite efficient for labeling and enrichment of 5hmC.

Encouraged by the above results, we set out to examine whether labeling and enrichment could also be achieved after adding hairpin adapters to obtain 5hmC-based circular DNA for the CAICas12a assay (Figure 2A). As illustrated in Figure 2B, phosphorylated DNA possessing an A tail could be connected to two phosphorylated adapters with T tails, which exhibit a hairpin structure. This configuration facilitated the formation of a template for subsequent rolling ring expansion, thereby addressing the limitations associated with DNA sequences and enabling further application to the genome. We first confirmed that the circular template of DNA containing 5hmC or NH$_2$-5hmC (Figure 2A) could be well amplified by RCA to exclude the steric effect of modifications resulting in no signal generation (Figure S5). The connection efficiency between DNA and adaptors was a key consideration. We optimized several factors that influenced the connection efficiency, including the PEG concentration and the ratio of adaptors to DNA. PEG could act as a macromolecular crowding agent, ultimately increasing the effective concen-

https://doi.org/10.1021/acssensors.4c03312
ACS Sens. 2025, 10, 2073−2079

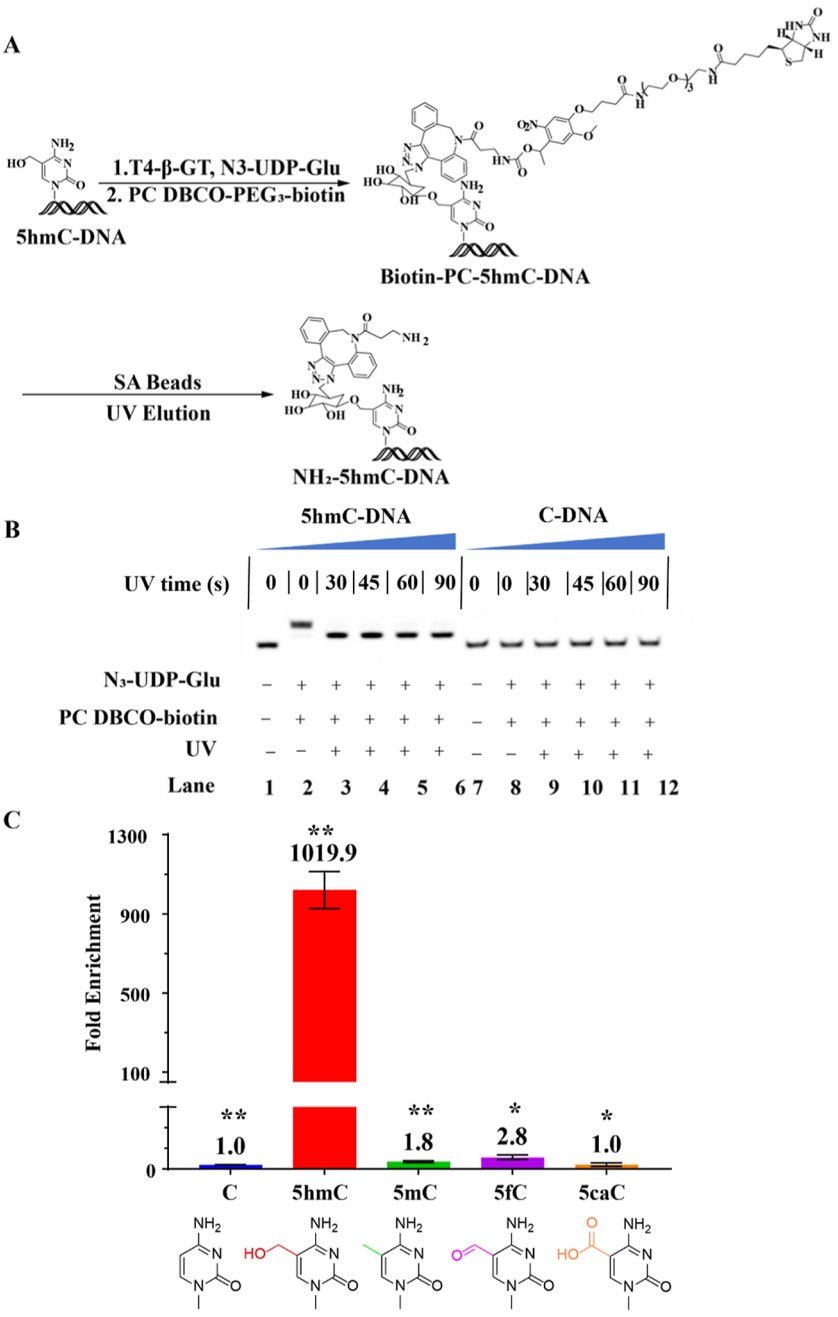


Figure 1. Specific labeling and enrichment of 5hmC-DNA. (A) Scheme of 5hmC-DNA chemical labeling. (B) Denaturing PAGE analysis of chemical labeling of 5hmC-DNA, C-DNA, and UV photolytic results. (C) Enrichment analysis of labeled 5hmC-DNA by SA magnetic beads and UV elution. Error bars represented the standard deviation of the mean of three independent experiments ($n = 3$). A two-tailed t-test was performed to calculate the P values (**$P < 0.01$ and *$P < 0.05$).

tration of ligase and DNA substrate.[32,33] Taking into account the availability of artificial DNA samples, a 20 bp short double-stranded DNA was used as a DNA model. We screened a series of PEG4000 concentrations, 0%, 2.5%, 5%, 10%, and 20%, and verified the ligation efficiency by polyacrylamide gel electrophoresis (PAGE) (see Figure S6A). The gray values of the bands observed in PAGE at different PEG concentrations were quantitatively analyzed using both bar chart and line chart (refer to Figure S6B). It was found that a 10% PEG4000 concentration yielded the highest ligation product efficiency, achieving approximately 54%, while only 6.7% DNA remained unligated at this concentration. Therefore, we selected 10% PEG4000 for subsequent experiments. Additionally, the ratio of DNA to adapters emerged as a critical factor influencing the ligation efficiency. We tested various ratios ranging from 5:1 to 100:1 and validated the results of these ligation reactions by native gel electrophoresis (Figure S7A). The results of the gray value calculations for the bar chart and line chart presented in the PAGE results (Figure S7B) indicate that under 30:1, approximately 60.85% of the circular products were obtained, with only 1.88% of the free DNA remaining. Therefore, the ratio of adapters to DNA was established as 30:1. Furthermore, we evaluated different adaptors, specifically the SL Adapter and the NEB Next Adapter, to assess their connection yields (Figure S8A,B). The findings revealed that the NEB Next

https://doi.org/10.1021/acssensors.4c03312
ACS Sens. 2025, 10, 2073−2079

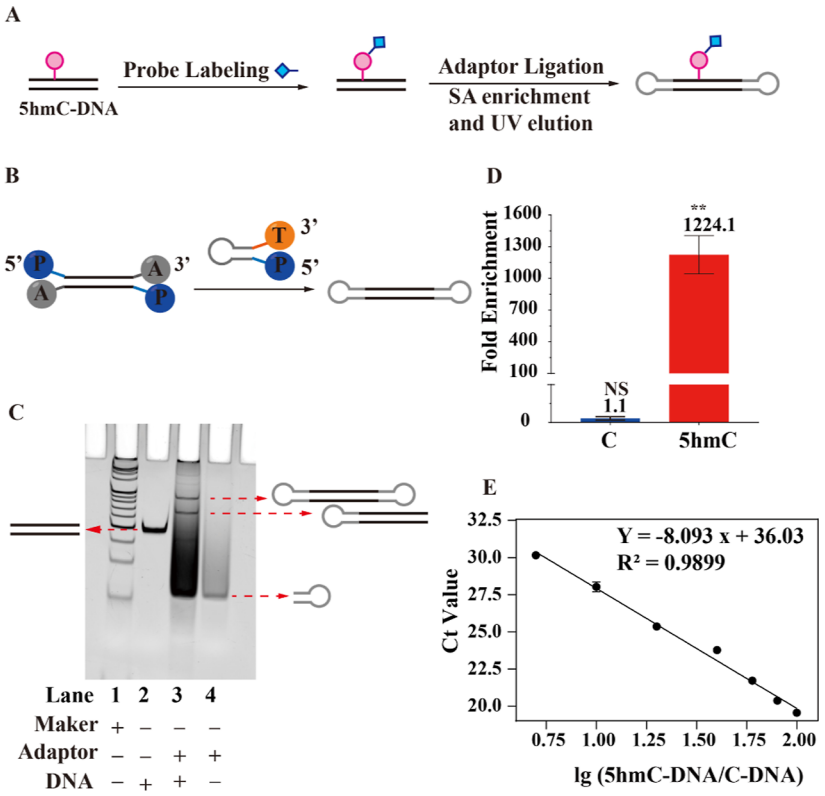


Figure 2. Enrichment of 5hmC-DNA after adaptor ligation. (A) Scheme of the design. (B) Schematic illustration of adaptor ligation. (C) Native PAGE analysis of adaptor ligation of 5hmC-DNA. (D) Enrichment analysis of cycled 5hmC-DNA compared with C-DNA. Error bars indicated the mean standard deviation of three independent experiments (n = 3). A two-tailed t test was performed to calculate the P values (**P < 0.01). (E) Linear analysis with diverse proportions of 5hmC-DNA/C-DNA from labeling to adaptor ligation. Error bars represented the mean standard deviation of three independent experiments (n = 3).

Adaptor demonstrated greater efficiency, resulting in a higher yield of circular products.

Considered that the actual length of the fragmented DNA sample is longer than 20 bp. We synthesized an 80 bp double-stranded DNA containing 5hmC through PCR and subsequently analyzed the ligation interactions between the 80 bp 5hmC DNA and hairpin adaptors using 12% native PAGE. As illustrated in Figure 2C, the results demonstrated the efficient connection between the 80 bp DNA and the adapters, with minimal free DNA observed in lane 3 of the native PAGE. We further investigated the potential for specific enrichment of cyclized 5hmC-DNA for subsequent Cas12a-coupled isothermal amplification. A comparison of the enrichment efficiency revealed that 5hmC-DNA exhibited significantly improved enrichment compared with C-DNA, as shown in Figure 2D, following adaptor ligation and quantification via qPCR. Additionally, we achieved a robust linear correlation in the fitting of curves using varying proportions of 5hmC-DNA to C-DNA (Figure 2E), with an R^2 value of 0.9925. These promising results provide a solid foundation for the subsequent accurate quantification of 5hmC.

We optimized the conditions influencing roll-ring amplification to demonstrate the efficiency of CAICas12a assays, as well as those related to Cas12a recognition and trans-cleavage activity. We examined the impact of phi29 DNA polymerase, primer concentration, fluorescence reporter, and Cas12a ribonucleoprotein (RNP) concentration on the overall fluorescence signal (see Figures S9–S12). Optimal concentrations for the final CAICas12a assays were identified. To balance fluorescent signal intensity with the cost-effectiveness of the entire system, phi29 DNA polymerase was selected at a concentration of 0.3 U/μL (Figure S9). The Cas12a RNP was chosen at a concentration of 1 nM (Figure S10), while the reporter probe was set at 500 nM (Figure S11). The primer concentration was established at 0.25 μM (Figure S12).

Under the relatively optimal conditions, we compared our method with that of the exponential RCA method. For comparison, various concentrations of 5hmC-DNA were used. Figure 3 displays the excellent sensitivity of CAICas12a assays. Even in the case of exponential amplification of double primers, the RCA method produced an effective signal above 10 pM at most (Figure 3A), while our assay could overcome this challenge and provide sensitive detection of as low as 100 fM using the protocol yet to be optimized (Figure 3B). The excellent detection sensitivity of the CAICas12a assay might be due to the excellent amplification performance of RCA as well as the highly sensitive targeting recognition ability of CRISPR-Cas12a.

Having demonstrated the excellent sensitivity of our CAICas 12a assay for 5hmC-DNA, the analytical capability of the CAICas 12a assay was systematically calibrated by different dilutions of synthetic 80 bp 5hmC-DNA according to the optimized protocol. Figure 4A shows the typical curves of real-time detection for 1.5 h and demonstrated a good fluorescence signal gradient with the 5hmC-DNA concentration varied from 6.38 pM to 50 fM. By calculating the fluorescence change rate at 90 min (ΔRFU), the lowest detectable dose (LOD) was found to be 11 fM, with a linear range from 6.38 to 50 fM. (Y = 21.05X + 4.467. R^2 = 0.9959, Figure 4B) at 90 minutes could be reached. The reliability of the CAICas12a assay was

https://doi.org/10.1021/acssensors.4c03312
ACS Sens. 2025, 10, 2073−2079

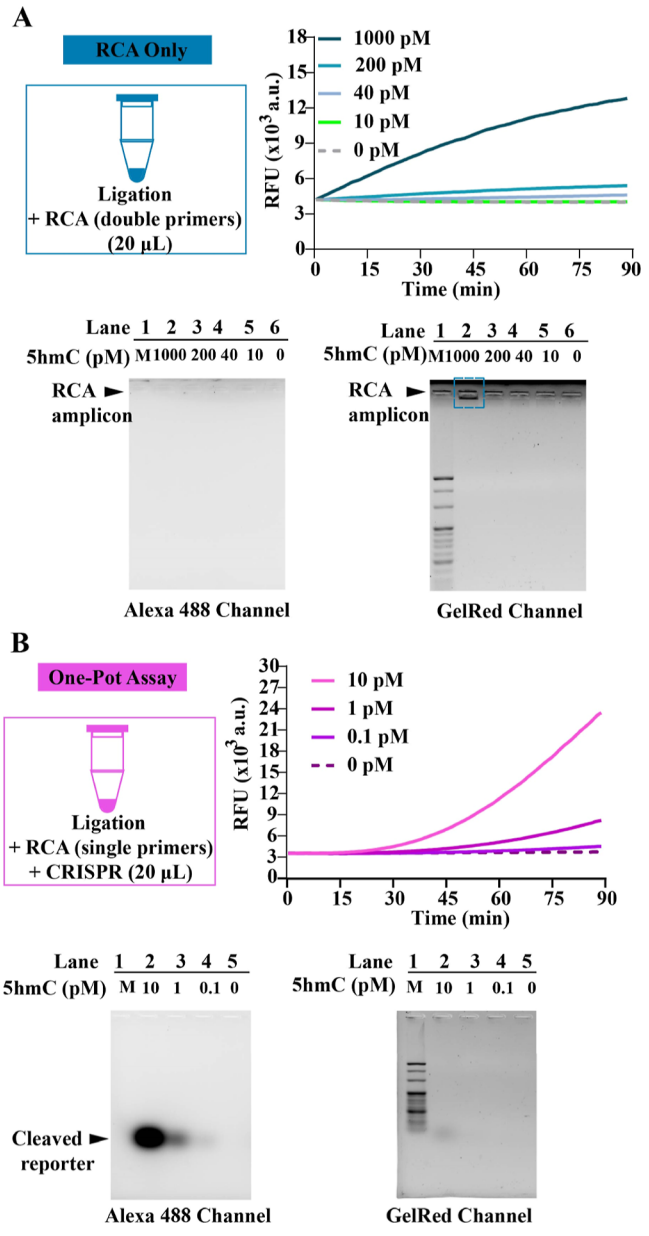


Figure 3. RCA, CAICas12a assay kinetics, and detection sensitivity comparison. (A) RCA-only method involved two sequential reactions of ligation and index RCA and could only detect higher than 10 pM 5hmC-DNA. (B) CAICas12a assays improved the sensitivity as low as 100 fM 5hmC-DNA without full optimization.

evaluated through the implementation of recovery experiments. Three DNA samples with varying degrees of 5hmC-DNA content, ranging from 0.75 to 2.25 nM, were analyzed in three times. And the results showed 92.5−108.3% recovery with small relative standard deviations of 2.6−5.8% (Table S2). The detection deviation might cause the recovery over 100%. However, in comparison to previously reported works,[34,35] the Cas12a assay exhibits superior assay accuracy.

The CAICas12a assay feasibility to analyze the biological sample was subjected to further investigation (Figure 5A). First, different types of colorectal cancer cells, specifically HCT116 and SW480, along with NCM460 were tested. To evaluate the quantitative accuracy of our methodology, we employed a commercial ELISA kit (ZYMO RESEARCH, USA) to quantify 5hmC levels in advance. The global 5hmC

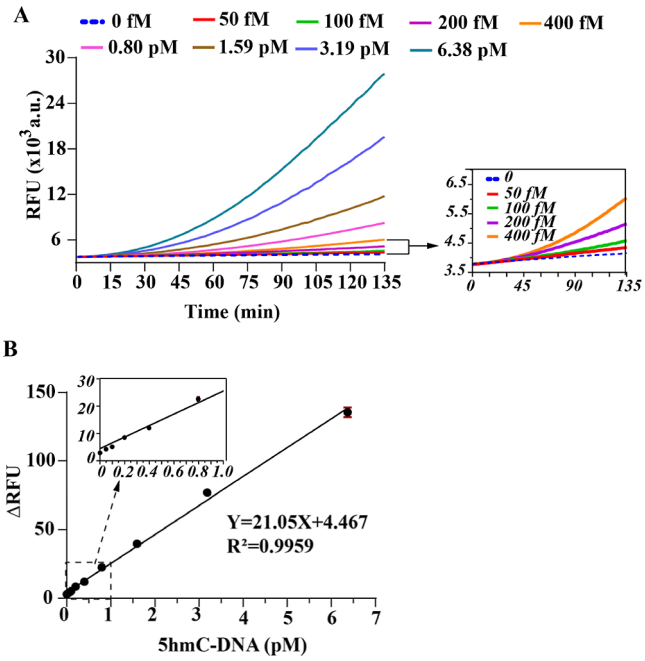


Figure 4. (A) Real-time curves for calibrating the assay with different synthetic 5hmC-DNA standard dilutions by an optimized method. Inset: the curves of averaged signal for 0 (NC), 50 and 100, 200, and 400 fM with 1 s.d. (n = 4). (B) Optimal assay time of 90 min yielded a linear calibration with a limit of detection (LOD) of 11 fM 5hmC-DNA, calculated from three times the standard deviation (s.d.) of the background level and a linear range from 6.38 pM to 50 fM. The standard deviation of the error bars is 1 s.d. (n = 4).

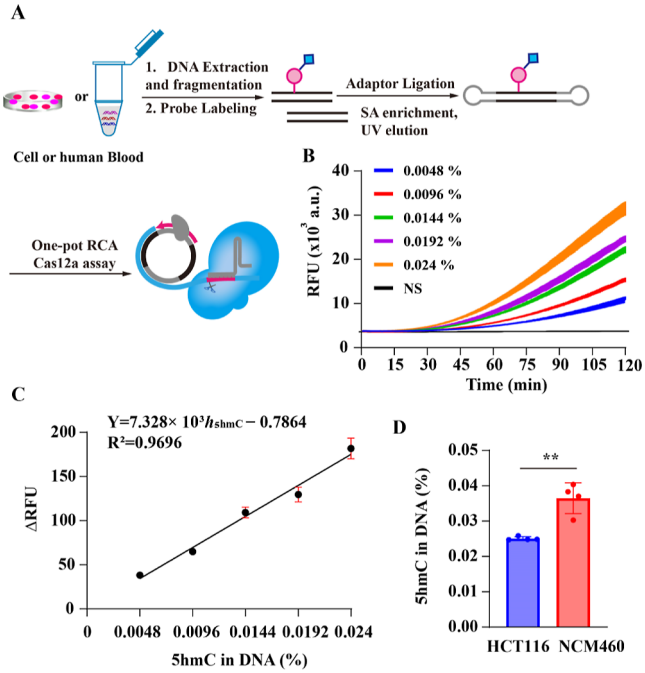


Figure 5. Biological sample analysis. (A) CAICas12a assay of the dsDNA fragments from biological samples. (B) Real-time curves for calibrating the CAICas12a assay with different dilutions of 5hmC-DNA from cell SW480. Error bars, 1 s.d. (n = 4). (C) Quantitative calibration plots for 5hmC in cell SW480. Error bars represent 1 s.d. (n = 4). (D) Global 5hmC levels in cell NCM 460 and HCT116. Error bars represent 1 s.d. (n = 4, $^{**}P < 0.01$).

https://doi.org/10.1021/acssensors.4c03312
ACS Sens. 2025, 10, 2073−2079

quantified by ELISA for SW480 was 0.024%. The ΔRFU exhibited a linear increase in correlation with the 5hmC content within the range of 0.0048−0.024% (Figure 5B), with a linear correlation of $\Delta RFU = 7.328 \times 10^3 h_{5hmC} - 0.7864$, $R^2 = 0.9696$ (Figure 5C). The quantitative calibration plot, with linear range encompassing the 5hmC content typically observed in most biological samples, was formulated based on the entire genomic sequence. Consequently, this plot was appropriate to quantify 5hmC levels in different genomic DNA samples derived from biological sources.

The levels of 5hmC were 0.025% per dN in DNA for HCT116 and 0.037% for NCM460, respectively (Figure 5D). The results obtained from CAICas12a are well consistent with the standard ELISA-based method (Table S3), The 5-hmC amount obtained by this assay in cell HCT116 was 0.025% of total DNA, which is similar to that analyzed by immunoassay (0.01−0.03% of total DNA).[8] Thus, this result provides supporting evidence for the high detection accuracy of the CAICas12a assay.

CONCLUSIONS

The current study develops a novel CAICas12a strategy for sensitively quantifying the global levels of 5hmC with nanogram-scale sample input. This quantification is particularly challenging with existing methodologies when the input DNA content was minimal, as is often the case with biological fluids such as blood, cerebrospinal fluid, and urine. The CAICas12a assay is reliable, cost-effective, and convenient. Multiple samples can be analyzed simultaneously on one plate with standard laboratory equipment. Furthermore, this strategy also represents a promising avenue for analysis of a multitude of samples containing 5hmC and other nucleoside modifications.

ASSOCIATED CONTENT

Supporting Information

The Supporting Information is available free of charge at https://pubs.acs.org/doi/10.1021/acssensors.4c03312.

All the sequences used in this work, chemical structural of the probe, MS characterization data, optimization experiment, original representative fluorescent curves, precision and recoveries of CAICas12a assay, and estimation of 5hmC in biological samples by ELISA and CAICas12a assay (PDF)

AUTHOR INFORMATION

Corresponding Authors

Chaoxing Liu − *Guangdong Provincial Key Laboratory of Digestive Cancer Research, Digestive Diseases Center, Scientific Research Center, The Seventh Affiliated Hospital of Sun Yat-sen University, Shenzhen, Guangdong 518107, P. R. China*; orcid.org/0000-0003-3077-9660; Email: liuchx69@mail.sysu.edu.cn

Zhaofan Luo − *Department of Clinical Laboratory, The Seventh Affiliated Hospital of Sun Yat-sen University, Shenzhen, Guangdong 518107, P. R. China*; Email: luozhaof@mail.sysu.edu.cn

Authors

Guangrong Zou − *Department of Clinical Laboratory, The Seventh Affiliated Hospital of Sun Yat-sen University, Shenzhen, Guangdong 518107, P. R. China*

Penglong Si − *Guangdong Provincial Key Laboratory of Digestive Cancer Research, Digestive Diseases Center, Scientific Research Center, The Seventh Affiliated Hospital of Sun Yat-sen University, Shenzhen, Guangdong 518107, P. R. China*

Jiaqi Wang − *Guangdong Provincial Key Laboratory of Digestive Cancer Research, Digestive Diseases Center, Scientific Research Center, The Seventh Affiliated Hospital of Sun Yat-sen University, Shenzhen, Guangdong 518107, P. R. China*

Meihua Yang − *School of Medicine, Sun Yat-sen University, Shenzhen, Guangdong 518107, P. R. China*

Jie Chen − *School of Medicine, Sun Yat-sen University, Shenzhen, Guangdong 518107, P. R. China*

Complete contact information is available at: https://pubs.acs.org/10.1021/acssensors.4c03312

Author Contributions

[‖]G.Z., P.S., and J.W. contributed equally to this work. The manuscript was written through the contributions of all authors.

Notes

The authors declare no competing financial interest.

ACKNOWLEDGMENTS

This work was supported by the National Key Research and Development Program of China (2022YFE0201800), the National Natural Science Foundation of China (22307150), the Guangdong Basic and Applied Basic Research Foundation (2024A1515012319), the Shenzhen Science and Technology Program (JCYJ20230807110315032 and JCYJ20240813150427036), and the China Postdoctoral Science Foundation (2024M753717).

REFERENCES

(1) Fabyanic, E. B.; Hu, P.; Qiu, Q.; Berríos, K. N.; Connolly, D. R.; Wang, T.; Flournoy, J.; Zhou, Z.; Kohli, R. M.; Wu, H. Joint single-cell profiling resolves 5mC and 5hmC and reveals their distinct gene regulatory effects. *Nat. Biotechnol.* **2024**, *42* (6), 960−974.

(2) Luo, C.; Hajkova, P.; Ecker, J. R. Dynamic DNA methylation: In the right place at the right time. *Science* **2018**, *361* (6409), 1336−1340.

(3) Cai, J.; Chen, L.; Zhang, Z.; Zhang, X.; Lu, X.; Liu, W.; Shi, G.; Ge, Y.; Gao, P.; Yang, Y.; et al. Genome-wide mapping of 5-hydroxymethylcytosines in circulating cell-free DNA as a non-invasive approach for early detection of hepatocellular carcinoma. *Gut* **2019**, *68* (12), 2195−2205.

(4) Li, W.; Zhang, X.; Lu, X.; You, L.; Song, Y.; Luo, Z.; Zhang, J.; Nie, J.; Zheng, W.; Xu, D.; et al. 5-Hydroxymethylcytosine signatures in circulating cell-free DNA as diagnostic biomarkers for human cancers. *Cell Res.* **2017**, *27* (10), 1243−1257.

(5) Jin, S. G.; Jiang, Y.; Qiu, R.; Rauch, T. A.; Wang, Y.; Schackert, G.; Krex, D.; Lu, Q.; Pfeifer, G. P. 5-Hydroxymethylcytosine is strongly depleted in human cancers but its levels do not correlate with IDH1 mutations. *Cancer Res.* **2011**, *71* (24), 7360−7365.

(6) Lian, C. G.; Xu, Y.; Ceol, C.; Wu, F.; Larson, A.; Dresser, K.; Xu, W.; Tan, L.; Hu, Y.; Zhan, Q.; et al. Loss of 5-hydroxymethylcytosine is an epigenetic hallmark of melanoma. *Cell* **2012**, *150* (6), 1135−1146.

(7) Chang, W.; Zhang, Z.; Jia, B.; Ding, K.; Pan, Z.; Su, G.; Zhang, W.; Liu, T.; Zhong, Y.; He, G.; et al. A 5-Hydroxymethylcytosine-Based Noninvasive Model for Early Detection of Colorectal Carcinomas and Advanced Adenomas: The METHOD-2 Study. *Clin. Cancer Res.* **2024**, *30* (15), 3337−3348.

(8) Li, W.; Liu, M. Distribution of 5-hydroxymethylcytosine in different human tissues. *J. Nucleic Acids* **2011**, *2011* (1), 870726.
(9) Liu, J.; Jiang, J.; Mo, J.; Liu, D.; Cao, D.; Wang, H.; He, Y.; Wang, H. Global DNA 5-Hydroxymethylcytosine and 5-Formylcytosine Contents Are Decreased in the Early Stage of Hepatocellular Carcinoma. *Hepatology* **2019**, *69* (1), 196−208.
(10) Vasanthakumar, A.; Godley, L. A. 5-hydroxymethylcytosine in cancer: significance in diagnosis and therapy. *Cancer Genet.* **2015**, *208* (5), 167−177.
(11) Kriaucionis, S.; Heintz, N. The nuclear DNA base 5-hydroxymethylcytosine is present in Purkinje neurons and the brain. *Science* **2009**, *324* (5929), 929−930.
(12) Song, C. X.; Yin, S.; Ma, L.; Wheeler, A.; Chen, Y.; Zhang, Y.; Liu, B.; Xiong, J.; Zhang, W.; Hu, J.; et al. 5-Hydroxymethylcytosine signatures in cell-free DNA provide information about tumor types and stages. *Cell Res.* **2017**, *27* (10), 1231−1242.
(13) Ito, S.; Shen, L.; Dai, Q.; Wu, S. C.; Collins, L. B.; Swenberg, J. A.; He, C.; Zhang, Y. Tet proteins can convert 5-methylcytosine to 5-formylcytosine and 5-carboxylcytosine. *Science* **2011**, *333* (6047), 1300−1303.
(14) Tahiliani, M.; Koh, K. P.; Shen, Y.; Pastor, W. A.; Bandukwala, H.; Brudno, Y.; Agarwal, S.; Iyer, L. M.; Liu, D. R.; Aravind, L.; et al. Conversion of 5-methylcytosine to 5-hydroxymethylcytosine in mammalian DNA by MLL partner TET1. *Science* **2009**, *324* (5929), 930−935.
(15) Kinney, S. M.; Chin, H. G.; Vaisvila, R.; Bitinaite, J.; Zheng, Y.; Estève, P. O.; Feng, S.; Stroud, H.; Jacobsen, S. E.; Pradhan, S. Tissue-specific distribution and dynamic changes of 5-hydroxymethylcytosine in mammalian genomes. *J. Biol. Chem.* **2011**, *286* (28), 24685−24693.
(16) Szwagierczak, A.; Bultmann, S.; Schmidt, C. S.; Spada, F.; Leonhardt, H. Sensitive enzymatic quantification of 5-hydroxymethylcytosine in genomic DNA. *Nucleic Acids Res.* **2010**, *38* (19), No. e181.
(17) Ko, M.; Huang, Y.; Jankowska, A. M.; Pape, U. J.; Tahiliani, M.; Bandukwala, H. S.; An, J.; Lamperti, E. D.; Koh, K. P.; Ganetzky, R.; et al. Impaired hydroxylation of 5-methylcytosine in myeloid cancers with mutant TET2. *Nature* **2010**, *468* (7325), 839−843.
(18) Hore, T. A.; von Meyenn, F.; Ravichandran, M.; Bachman, M.; Ficz, G.; Oxley, D.; Santos, F.; Balasubramanian, S.; Jurkowski, T. P.; Reik, W. Retinol and ascorbate drive erasure of epigenetic memory and enhance reprogramming to naïve pluripotency by complementary mechanisms. *Proc. Natl. Acad. Sci. U.S.A.* **2016**, *113* (43), 12202−12207.
(19) Wu, H.; Zhang, Y. Charting oxidized methylcytosines at base resolution. *Nat. Struct. Mol. Biol.* **2015**, *22* (9), 656−661.
(20) Liu, Y.; Siejka-Zielińska, P.; Velikova, G.; Bi, Y.; Yuan, F.; Tomkova, M.; Bai, C.; Chen, L.; Schuster-Böckler, B.; Song, C. X. Bisulfite-free direct detection of 5-methylcytosine and 5-hydroxymethylcytosine at base resolution. *Nat. Biotechnol.* **2019**, *37* (4), 424−429.
(21) Chen, J. S.; Ma, E.; Harrington, L. B.; Da Costa, M.; Tian, X.; Palefsky, J. M.; Doudna, J. A. CRISPR-Cas12a target binding unleashes indiscriminate single-stranded DNase activity. *Science* **2018**, *360* (6387), 436−439.
(22) Song, X.; Liu, C.; Wang, N.; Huang, H.; He, S.; Gong, C.; Wei, Y. Delivery of CRISPR/Cas systems for cancer gene therapy and immunotherapy. *Adv. Drug Delivery Rev.* **2021**, *168*, 158−180.
(23) Huang, W.; Wang, J.; Wang, C.; Liu, Y.; Li, W.; Chen, Q.; Zhai, J.; Xiang, Z.; Liu, C. Expanding Cas12a Activity Control with an RNA G-Quadruplex at the 5′ end of CRISPR RNA. *Adv. Sci.* **2025**, *12* (7), e2411305.
(24) Kaminski, M. M.; Abudayyeh, O. O.; Gootenberg, J. S.; Zhang, F.; Collins, J. J. CRISPR-based diagnostics. *Nat. Biomed. Eng.* **2021**, *5* (7), 643−656.
(25) Li, Y.; Li, S.; Wang, J.; Liu, G. CRISPR/Cas Systems towards Next-Generation Biosensing. *Trends Biotechnol.* **2019**, *37* (7), 730−743.
(26) Gootenberg, J. S.; Abudayyeh, O. O.; Lee, J. W.; Essletzbichler, P.; Dy, A. J.; Joung, J.; Verdine, V.; Donghia, N.; Daringer, N. M.; Freije, C. A.; et al. Nucleic acid detection with CRISPR-Cas13a/C2c2. *Science* **2017**, *356* (6336), 438−442.
(27) Joung, J.; Ladha, A.; Saito, M.; Kim, N. G.; Woolley, A. E.; Segel, M.; Barretto, R. P. J.; Ranu, A.; Macrae, R. K.; Faure, G.; et al. Detection of SARS-CoV-2 with SHERLOCK One-Pot Testing. *N. Engl. J. Med.* **2020**, *383* (15), 1492−1494.
(28) Li, L.; Li, S.; Wu, N.; Wu, J.; Wang, G.; Zhao, G.; Wang, J. HOLMESv2: A CRISPR-Cas12b-Assisted Platform for Nucleic Acid Detection and DNA Methylation Quantitation. *ACS Synth. Biol.* **2019**, *8* (10), 2228−2237.
(29) Li, Y.; Yang, X.; Dong, Y.; Wang, J.; Liu, C. CRISPR−Cas12a detection of DNA glycosylases via DNA modification switching. *Chem. Commun.* **2024**, *60* (86), 12569−12572.
(30) Hu, M.; Wang, Y.; Zhou, X. Photochemical regulatory strategies for nucleic acid function and their biomedical applications. *Interdiscip. Med.* **2024**, *2* (3), No. e20240006.
(31) Song, C. X.; Szulwach, K. E.; Fu, Y.; Dai, Q.; Yi, C.; Li, X.; Li, Y.; Chen, C. H.; Zhang, W.; Jian, X.; et al. Selective chemical labeling reveals the genome-wide distribution of 5-hydroxymethylcytosine. *Nat. Biotechnol.* **2011**, *29* (1), 68−72.
(32) Harrison, B.; Zimmerman, S. B. T4 polynucleotide kinase: Macromolecular crowding increases the efficiency of reaction at DNA termini. *Anal. Biochem.* **1986**, *158* (2), 307−315.
(33) Xiao, F.; Wang, Q.; Zhang, K.; Liu, C.; Zou, G.; Zhou, X. Oxime formation coordination-directed detection of genome-wide thymine oxides with nanogram-scale sample input. *Chem. Sci.* **2022**, *13* (31), 9074−9078.
(34) Guo, M.; Zhang, L.; Du, Y.; Du, W.; Liu, D.; Guo, C.; Pan, Y.; Tang, D. Enrichment and Quantitative Determination of 5-(Hydroxymethyl)-2′-deoxycytidine, 5-(Formyl)-2′-deoxycytidine, and 5-(Carboxyl)-2′-deoxycytidine in Human Urine of Breast Cancer Patients by Magnetic Hyper-Cross-Linked Microporous Polymers Based on Polyionic Liquid. *Anal. Chem.* **2018**, *90* (6), 3906−3913.
(35) Xia, X.; Wang, Y.; Yang, H.; Dong, Y.; Zhang, K.; Lu, Y.; Deng, R.; He, Q. Enzyme-free amplified and ultrafast detection of aflatoxin B(1) using dual-terminal proximity aptamer probes. *Food Chem.* **2019**, *283*, 32−38.

https://doi.org/10.1021/acssensors.4c03312
ACS Sens. 2025, 10, 2073−2079